Synthesis and vibrational spectroscopic characterisation of synthetic hydrozincite and smithsonite

Matthew C. Hales, Ray L. Frost[•]

Inorganic Materials Research Program, School of Physical and Chemical Sciences, Queensland University of Technology, GPO Box 2434, Brisbane Queensland 4001, Australia.

Abstract

Hydrozincite and smithsonite were synthesised by controlling the partial pressure of CO_2. Previous crystallographic studies concluded that the structure of hydrozincite was a simple one. However both Raman and infrared spectroscopy show that this conclusion is questionable. Multiple bands are observed in both the Raman and infrared spectra in the $(CO_3)^{2-}$antisymmetric stretching and bending regions of hydrozincite showing that the symmetry of the carbonate anion is reduced and in all probability the carbonate anions are not equivalent in the hydrozincite structure. Multiple OH stretching vibrations centred in both the Raman and infrared spectra show that the OH units in the hydrozincite structure are non-equivalent. The Raman spectrum of synthetic smithsonite is a simple spectrum characteristic of carbonate with Raman bands observed at 1408, 1092 and 730 cm^{-1}.
The symmetry of the carbonate anion in hydrozincite is C_{2v} or C_s. This symmetry reduction results in multiple bands in both the symmetric stretching and bending regions. The intense band of hydrozincite at 1062 cm^{-1} is assigned to the ν_1 $(CO_3)^{2-}$ symmetric stretching mode. Three Raman bands assigned to the ν_3 $(CO_3)^{2-}$ antisymmetric stretching modes are observed for hydrozincite at 1545, 1532 and 1380 cm^{-1}. Multiple infrared or Raman bands are observed in 800 to 850 cm^{-1} and 720 to 750 cm^{-1} regions and are attributed to ν_2 and ν_4 bending modes confirming the reduction of the carbonate anion symmetry in the hydrozincite structure. A Raman band for hydrozincite at 980 cm^{-1} is attributed to the δ OH deformation mode.

Key words: hydrozincite, smithsonite; rosasite; hydroxy carbonates; synthesis, infrared and Raman spectroscopy

1. Introduction

Hydrozincite $Zn_5(CO_3)_2(OH)_6$ is a mineral formed in the oxidised zones of zinc deposits and is found as masses or crusts and is often not readily observed and may be confused with other minerals such as calcite [1]. The mineral is often associated with other minerals such as smithsonite, calcite, hemimorphite, aurichalcite [1]. Smithsonite is naturally occuring zinc carbonate [1]. It is hexagonal with point group 3bar 2/m. The mineral is named for James Smithson, the founder of the Smithsonian Institution (USA). The mineral is reknowned for its pearly lustre and comes in a range of colours which vary across all colours of the visible spectrum. Although it must be stated that no studies have been undertaken to explain the colours

[•] Author to whom correspondence should be addressed (r.frost@qut.edu.au)

of the minerals even though chemical analyses of the coloured smithsonites have been undertaken. Carbonates with intermediate sized divalent cations normally crystallise in the calcite structure [2]. Those with larger cations have an aragonite type structure. Hydrozincite is not commonly found as a crystalline material. Some lathelike or bladed crystals may be uncommonly found. The mineral is flattened on 100 and elongated on 001 with pointed terminations up to 6 mm in length. The mineral is monoclinic with Space Group: C 2/m and point group 2/m [3-5]. Some considerations of the stacking in the crystals have been made [4]. A model of the structure of hydrozincite is given in Figure 1. This figure displays the structure of hydrozincite looking along the a, b and c axes, respectively.

It is important to study the malachite-hydrozincite-hydrocerrusite assemblage and the stability of the system. The reason is that these minerals are the stable minerals at one atmosphere. One essential method is to use vibrational spectroscopic techniques. Infrared and Raman spectroscopy have been used to investigate carbonates including azurite and malachite [6, 7]. A detailed single crystal Raman study of selected mineral carbonates has been undertaken [6, 8]. This would seem important in the context of the stability of the hydroxy carbonates of Zn, Cu and Pb. However the vibrational spectroscopy of hydrozincite has not been undertaken. This may be due to the amorphous nature of the hydrozincite crusts. Few infrared spectral studies of related minerals such as the rosasite group have been forthcoming [7, 9-11]. An infrared stretching vibration of the hydroxyl unit of azurite was observed at 3425 cm^{-1}, whereas two bands were reported for malachite at 3400 and 3320 cm^{-1}. The observation of two bands for malachite suggests coupling of the hydroxyl stretching vibrations [8]. This coupling was not observed for azurite [8]. Azurite and malachite form the basis of pigments in samples of an archaeological or medieval nature [12-15]. It is not known if hydrozincite was used in medieval paintings. Malachite has a characteristic infrared active intense band at ~430 cm^{-1} and for azurite an intense band at ~400 cm^{-1}. The deformation modes of azurite were reported at 1035 and 952 cm^{-1} and at 1045 and 875 cm^{-1} for malachite. [7, 16] Hydrozincites from different origins showed differences in the infrared spectra in the OH stretching region [4]. These variations were accounted for by differences in stacking of the minerals [4]. Minerals in the rosasite mineral group, (a group of copper hydroxy carbonates) namely, rosasite, glaukosphaerite, kolwezite, mcguinnessite, nullaginite and pokrovskite have been studied by Raman spectroscopy at 298 and 77 K [17, 18].

Vibrational spectroscopic studies of carbonate minerals have been undertaken over an extended period of time [19-21]. Adler and Kerr showed that differences in the infrared absorption spectra of carbonates were a function of cation size [19]. Some NIR studies have been undertaken [22, 23] . Raman studies also have been forthcoming but not in recently [24-26]. Farmer reported the vibrational wavenumbers of calcite structured minerals (table 12. IX page 239) [2]. In this table the band positions for smithsonite were listed as 1093 cm^{-1} (ν_1 symmetric stretching mode), 1412 and 1440 cm^{-1} (ν_3 antisymmetric stretching mode), 870 cm^{-1} (ν_2 in-plane bending mode), 733 and 743 cm^{-1} (ν_4 out of plane bending mode) with lattice modes at 307, 200, 165 cm^{-1}. Some variation of band positions is found in the literature. Very little spectroscopic information on hydrozincite is available. However a comparison may be made with the mineral aurichalcite. The mineral aurichalcite $(Zn,Cu^{2+})_5(CO_3)_2(OH)_6$ is also monoclinic as are many of the other hydroxy

carbonates such as malachite [27-29]. Aurichalcite forms in the oxidation zones of zinc-copper deposits. Crystals are similar to that of hydrozincite and are acicular and fibrous and often found in aggregates. Anthony et al. (2003) reports aurichalcite to be acicular to lathlike crystals with prominent crystal growth along the [010] axis, commonly straited parallel to [001] axis. The mineral is of point group 2/*m* and space group $P2_1/m$ [1]. The accurate X-ray crystallography of aurichalcite is difficult to obtain because of its very small interwoven needles which makes obtaining single crystal studies difficult [1, 3, 29, 30]. Harding (1994) showed that the positions in the structure of aurichalcite are octahedrally coordinated. The atom positions occupied by zinc have tetrahedral coordination [3]. Spectroscopic studies of aurichalcites and related minerals such as hydrozincite have been sparse. Reports regarding the chemical analysis, ESR, electronic and some limited infrared spectroscopic studies have been published [31]. These workers reported optical spectra revealing the presence of copper in D_{4h} symmetry with crystal field (Dq) and tetragonal field (Ds and Dt). This research was further extended in a comparison of rosasite and aurichalcite [32]. Optical and EPR spectra of aurichalcite accounted for Cu^{2+} ion in the distorted octahedron site [32]. Stoilova et al. (2002) reported the infrared spectra of a series of synthetic hydroxy carbonates containing Cu^{2+} [33].

Raman spectroscopy has proven very useful for the study of minerals [34-36]. Indeed Raman spectroscopy has proven most useful for the study of diagentically related minerals often occuring with carbonate minerals [37-41]. Some previous studies have been undertaken by the authors using Raman spectroscopy to study complex secondary minerals formed by crystallisation from concentrated sulphate solutions [42]. The aim of this paper is to present Raman and infrared spectra of synthetic hydrozincites and smithsonite and to discuss the spectra from the structural point of view. The paper is a part of systematic studies of vibrational spectra of minerals of secondary origin in the oxide supergene zone and their synthetic analogs.

Experimental

Synthesis of hydrozinciteand smithsonite

Three different synthesis techniques were trialled during the synthesis of hydrozincite. The first involved weighing out equimolar amounts of the Zinc (II) salt and the carbonate salt, dissolving in a minimum volume of deionised water and combining rapidly in a beaker of adequate size. The two Zinc salts used in the experiment were zinc chloride $ZnCl_2$ and zinc nitrate $Zn(NO_3)_2$. Sodium hydrogen carbonate $NaHCO_3$ was the source of the carbonate ion used for both experiments. The following chemical reaction occurs:

$5ZnCl_2\,(s) + 10NaHCO_3(soln) \leftrightarrow Zn_5(CO_3)_2(OH)_6\,(s) + 8CO_2\,(g) + 10NaCl(soln) + 2H_2O$

Smithsonite is formed according to the following reaction:

$ZnCl_2\,(soln) + 2NaHCO_3(soln) \leftrightarrow ZnCO_3\,(s) + CO_2\,(g) + 2NaCl(soln) + H_2O$

The second experiment involved a similar process of mixing the reactants but at a controlled rate using a peristaltic pump system operating at 10cm min^{-1}. Both the zinc salt and carbonate salt were made up as standard solutions of equal concentration 0.5M so that adding equivalent volumes 50cm^3 of reagents gave the desired amounts of reagents according to the stoichiometry of the reaction. The pH of the reaction was

monitored but remained essentially constant at pH=7.2. The following alternative reaction is envisaged for the formation of smithsonite:

$Zn_5(CO_3)_2(OH)_6$ (s) + $3CO_2$ (g) ↔ $5ZnCO_3$ (s) +3 H_2O (g).

The third synthesis method involved hydro-thermally treating some of the products from the previous two methods in a hydrothermal bomb at 100°C for 48 hrs with adequate washing of the products after removal from the bomb. Adequate washing was achieved when the silver chloride test was negative. Thus indicating that all free chloride ions were removed. All of the samples were then washed and dried with ethanol and were placed in an oven at 80°C over night to dry thoroughly.

From the XRD analysis, it was found that there was an impurity of another synthetic mineral found in the samples that had both used zinc chloride and had then been hydro-thermally treated. It can be seen that hydrothermal treatment actually promotes the formation of this synthetic mineral identified as simonkolleite, a zinc chloride hydroxide hydrate mineral with the formula of $Zn_5(OH)_8Cl_2H_2O$. It is apparent that if the sample was synthesised using the $ZnCl_2$ and then hydro-thermally treated, the carbonate yield decreased significantly thereby increasing the yield of simonkolleite.

X-ray diffraction

XRD analyses were performed on a Philips PANalytical X'Pert PRO X-ray diffractometer (radius: 240.0 mm). Incident X-ray radiation was produced from a line focused PW3373/10 Cu X-ray tube, operating at 40 kV and 40 mA, providing a $K\alpha_1$ wavelength of 1.54 Å. The incident beam was monochromated through a 0.020 mm Ni filter then passed through a 0.04 rad. Soller slit, a 15 mm fixed mask and a ½° fixed anti scatter slit. After interaction with the sample, the diffracted beam passed though a secondary 0.04 rad. Soller slit and a 0.25° progressive divergence slit before detection by an X'Celerator RTMS detector. The detector was set in scanning mode, with an active length of 2.022 mm. Samples were analysed utilising Bragg-Brentano geometry over a range of 1.5 – 70° 2θ with a step size of 0.02° 2θ, with each step measured for 12.1 seconds. For all XRD analyses, the samples were dispersed in hexane and dropped onto low background quartz plates, forming a thin film upon evaporation of the hexane.

Raman microprobe spectroscopy

The crystals of hydrozincite or smithsonite were placed and oriented on the stage of an Olympus BHSM microscope, equipped with 10x and 50x objectives and part of a Renishaw 1000 Raman microscope system, which also includes a monochromator, a filter system and a Charge Coupled Device (CCD). Raman spectra were excited by a HeNe laser (633 nm) at a resolution of 2 cm^{-1} in the range between 100 and 4000 cm^{-1}. Repeated acquisition using the highest magnification was accumulated to improve the signal to noise ratio. Band positions were calibrated using the 520.5 cm^{-1} line of a silicon wafer. In order to ensure that the correct spectra are obtained, the incident excitation radiation was scrambled. Previous studies by the authors provide more details of the experimental technique [43-46].

2.3. Mid-IR spectroscopy

Infrared spectra were obtained using a Nicolet Nexus 870 FTIR spectrometer with a smart endurance single bounce diamond ATR cell. Spectra over the 4000–525 cm^{-1} range were obtained by the co-addition of 64 scans with a resolution of 4 cm^{-1} and a mirror velocity of 0.6329 cm/s. Spectra were co-added to improve the signal to noise ratio.

Spectral manipulation such as baseline adjustment, smoothing and normalisation were performed using the Spectracalc software package GRAMS (Galactic Industries Corporation, NH, USA). Band component analysis was undertaken using the Jandel 'Peakfit' software package, which enabled the type of fitting function to be selected and allows specific parameters to be fixed or varied accordingly. Band fitting was done with the lowest possible number of Lorentz-Gauss cross-product functions. The Lorentz-Gauss ratio was maintained at values greater than 0.7 and fitting was undertaken until reproducible results were obtained with squared correlations of r^2 greater than 0.995.

3. Results and discussion

Relative stability of hydrozincite and smithsonite

The relative stability of hydrozincite and smithsonite are of importance to understand their formation in nature. Of the secondary minerals containing zinc only smithsonite and hydrozincite are known. The formation of these minerals is controlled by the partial pressure of CO_2 [47, 48], according to the equation for the formation of hydrozincite with logK = 10.32 [47]. Thus ZnO is unstable with respect to hydrozincite at partial pressures above $10^{-5.16}$. If the partial pressure of CO_2 increases above $10^{-1.41}$ smithsonite formation is favoured according to the reaction $Zn_5(CO_3)_2(OH)_6$ (s) + $3CO_2$ (g) ↔ $5ZnCO_3$ (s) +3 H_2O (g). These results provide implications for the relative stability of hydrozincite and smithsonite. It is noted that hydrozincite may from from solutions resulting from oxidized zone of a Pb-Zn ore body [47]. Thus zincite (ZnO) is a rare mineral and smithsonite is only stable at elevated CO_2 partial pressures. The partial pressure range for the stability of hydrozincite according to Williams is limited and no doubt this accounts for the rarity of the mineral in nature [48]. The mineral can be readily synthesised in the laboratory and is often found in corrosion products of zinc [14, 29, 49]. In the presence of tenerite (CuO) the formation of malachite and/or azurite is favoured at the expense of hydrozincite [48]. Often the assembalge malachite-hydrozincite-hydrocerrusite is the stable system at 1 atmosphere CO_2 pressure. Bouchard and Smith reported the formation of a significant number of phases on metal coins including hydrozincite [14].

An impurity of simonkolleite with hydrozincite may be synthesised depending upon the starting materials. The conditions for the formation of simonkolleite are the same as that for hydrozincite. It was found that if zinc chloride was used in the synthesis and the sample was hydrothermally treated, a significant yield of simonkolleite was produced. The sample proved to be a mixed phase of simonkolleite and hydrozincite. It is also interesting that when smithsonite is formed, simonkolleite was not. The XRD patterns together with standard XRD reference patterns of

synthetic smithsonite and hydrozincite are shown in Figure 2. Clearly the pure hydrozincite and smithsonite phases were synthesised as single phases.

Spectroscopy

The Raman and infrared spectra of synthetic hydrozincite and smithsonite in the 550 to 1800 cm^{-1} region are shown in Figure 3. The results of the band component analysis are reported in Table 1. Raman bands are assigned according to published data and by comparison with data for other minerals [18, 45, 50-58]. The Raman spectrum of synthetic hydrozincite shows an intense sharp band at 1062 cm^{-1}. Other low intensity bands are observed at 1078 and 980 cm^{-1}. The latter Raman band at 980 cm^{-1} is assigned to the δ OH deformation mode. The Raman spectrum of synthetic smithsonite shows a sharp band at 1092 cm^{-1}. These bands are assigned to the ν_1 symmetric stretching mode of the carbonate unit. Infrared bands in this position are not observed for smithsonite. However a band at 1040 cm^{-1} is found in the infrared spectrum of synthetic hydrozincite. The $(CO_3)^{2-}$ ν_1 band of the hydrozincite compound should not be infrared active. However, because of symmetry reduction of the carbonate anion through distortion the infrared band becomes activated.

A number of low intensity Raman bands are observed in the 1300 to 1500 cm^{-1} region (Figure 3). A single band for synthetic smithsonite is observed at 1408 cm^{-1} and for hydrozincite bands at 1545 and 1380 cm^{-1} are found. These bands may be ascribed to the ν_3 $(CO_3)^{2-}$ antisymmetric stretching modes. In the infrared spectrum of synthetic smithsonite a broad spectral profile centred on 1392 cm^{-1} is observed and is assigned to the ν_3 $(CO_3)^{2-}$ antisymmetric stretching modes. In the infrared spectrum of synthetic hydrozincite bands are observed at 1505, 1383 and 1338 cm^{-1}. The difference in the number of bands in this spectral region of smithsonite and hydrozincite is ascribed to the symmetry reduction of the hydrozincite.

The ν_2 bending mode for carbonates varies from around 890 cm^{-1} to 850 cm^{-1} . For smithsonite Farmer reported an infrared band at 870 cm^{-1} [2]. For hydrozincite the infrared band was observed at 837 cm^{-1} [2]. In this work no Raman bands are observed for synthetic smithsonite or hydrozincite in this position. In the infrared spectrum of synthetic hydrozincite bands are observed at 888, 832 cm^{-1} with a broad feature at 799 cm^{-1}. In the infrared spectrum of smithsonite two bands are observed at 864 and 834 cm^{-1}. These bands are assigned to the carbonate ν_2 bending mode. The observation of more than one ν_2 mode suggests symmetry reduction of the carbonate anion in the structure. A comparison may be made with the spectra of other hydroxycarbonates. A mineral similar to hydrozincite is aurichalcite $(Zn,Cu)_5(CO_3)_2(OH)_6$. For aurichalcite two Raman bands may be resolved at 860 and 845 cm^{-1}. Only a single band at 817 cm^{-1} is observed in this region for malachite $Cu_2(CO_3)(OH)_2$. The FTI R spectrum of malachite showed two bands at 879 and 821 cm^{-1} [8]. This FTIR spectral region is more complex for azurite $Cu_3(CO_3)_2(OH)_2$ with bands observed at 872, 837, 815 and 796 cm^{-1}.

Multiple bands are observed for the carbonate ν_4 in phase bending modes in the Raman spectrum of hydrozincite with bands at 733, 707 and 636 cm^{-1}. The number of bands observed in this spectral region may be attributed to the structural distortion of the mineral. For smithsonite only a single band at 730 cm^{-1} is observed.

Farmer (based upon the work of Moenke [21]] reported two infrared bands for hydrozincite at 738 and 710 cm^{-1}[2]. Farmer also reported only a single band for smithsonite at 733 cm^{-1}. In the infrared spectrum of synthetic hydrozincite a broad complex spectral profile with two bands resolved at 737 and 707 cm^{-1} is observed. In the infrared spectrum of synthetic smithsonite two bands at 743 and 715 cm^{-1} are observed. It is interesting that in the Raman spectrum of aurichalicte three bands are observed at 752, 733 and 708 cm^{-1}. The equivalent Raman bands for malachite are observed at 752 and 717 cm^{-1}. In the infrared spectra bands are observed at 779, 754 and 701 cm^{-1} for azurite and at 780, 750 and 715 cm^{-1} for malachite [8].

In the Raman spectrum of smithsonite in the 100 to 600 cm^{-1} region, two prominent bands are observed at 304 and 198 cm^{-1} (Figure 4). These bands are assigned to lattice modes. Farmer reported lattice modes in the infrared spectrum of smithsonite at 307, 200 and 165 cm^{-1} [2]. For hydrozincite Raman bands are observed at 385, 346, 272 and 227 cm^{-1}. Bands in this spectral region have not been previously defined. The Raman spectra of the OH stretching region of the three aurichalcite mineral samples are shown in Figure 5. The Raman spectrum of smithsonite shows two bands at 3472 and 3265 cm^{-1} and the infrared spectrum a single band at 3356 cm^{-1}. These bands are attributed to adsorbed water. For synthetic hydrozincite infrared bands are observed at 3291, 3063 and 2895 cm^{-1} and Raman bands are found at 3541, 3407, 3286 cm^{-1}. Farmer based upon the work of Moenke reported bands for hydrozincite at 3300 and 3260 cm^{-1}. A single symmetric band is observed for aurichalcite at 3338 cm^{-1}. A comparison can be made with rosasite where two distinct bands are observed at 3387 and 3319 cm^{-1}. The bands are assigned to the OH stretching vibration. Bouchard and Smith (2003) reported a noticeably broad band in the Raman spectrum of aurichalcite at 3331 cm^{-1}. This value is in good agreement with the results reported in this work. Infrared bands for aurichalcite are observed at 3491, 3350, 3244 and a broad band at 3173 cm^{-1}. The infrared spectrum of a second aurichalcite mineral gave bands at 3359, 3249 and 3106 cm^{-1}. The broad band at around 3163 cm^{-1} may be ascribed to adsorbed water. The first two bands are assigned to OH stretching vibrations.

Conclusions

Of the secondary minerals of zinc only two minerals are known, namely smithsonite and hydrozincite and their formation of is controlled by the partial pressure of CO_2 according to the reactions
$5ZnO(s) + 2\ CO_2\ (g) \leftrightarrow Zn_5(CO_3)_2(OH)_6\ (s)$ and
$Zn_5(CO_3)_2(OH)_6\ (s) + 3CO_2\ (g) \leftrightarrow 5ZnCO_3\ (s) + 3\ H_2O\ (g)$. An impurity of simonkolleite with hydrozincite was synthesised depending upon the starting materials

The Raman spectra of synthetic hydrozincite and smithsonite show intense sharp bands at 1062 and 1092 cm^{-1}, assigned to the ν_1 symmetric stretching mode of carbonate. Raman bands for synthetic smithsonite is observed at 1408 cm^{-1} and for hydrozincite bands at 1545 and 1380 cm^{-1} and are ascribed to the ν_3 $(CO_3)^{2-}$ antisymmetric stretching modes. Multiple bands are observed for the carbonate ν_4 in phase bending modes in the Raman spectrum of hydrozincite with bands at 733, 707 and 636 cm^{-1}. The number of bands observed in this spectral region may be attributed to the structural distortion of the mineral. For smithsonite only a single band at 730

cm^{-1} is observed. No Raman bands are observed for synthetic smithsonite or hydrozincite around 850 cm^{-1}. This is the expected position of the ν_2 mode. In the infrared spectrum of synthetic hydrozincite bands are observed at 888, 832 cm^{-1} with a broad feature at 799 cm^{-1}.

Acknowledgments

The financial and infra-structure support of the Queensland University of Technology, Inorganic Materials Research Program is gratefully acknowledged. The Australian Research Council (ARC) is thanked for funding the instrumentation.

References

[1] J.W. Anthony, R.A. Bideaux, K.W. Bladh, M.C. Nichols, Handbook of Mineralogy, Mineral Data Publishing, Tiscon, Arizona, USA, 2003.
[2] V.C. Farmer, Mineralogical Society Monograph 4: The Infrared Spectra of Minerals, 1974.
[3] M.M. Harding, B.M. Kariuki, R. Cernik, G. Cressey, Acta Crystallographica, Section B: Structural Science B50 (1994) 673-676.
[4] W. Zabinski, Canadian Mineralogist 8 (1966) 649-652.
[5] S. Ghose, Acta Cryst. 17 (1964) 1051-1057.
[6] J.A. Goldsmith, S.D. Ross, Spectrochimica Acta, Part A: Molecular and Biomolecular Spectroscopy 24 (1968) 2131-2137.
[7] C. Rodriguez P, Boletin de la Sociedad Quimica del Peru 35 (1969) 38-55.
[8] R.L. Frost, W.N. Martens, L. Rintoul, E. Mahmutagic, J.T. Kloprogge, J. Raman Spectrosc. 33 (2002) 252-259.
[9] K. Wada, Kanzei Chuo Bunsekishoho 19 (1978) 133-187.
[10] P. Tarte, Proc. Intern. Meeting Mol. Spectry., 4th, Bologna, 1959 3 (1962) 1041-1049.
[11] P. Tarte, M. Deliens, Bulletin de la Societe Royale des Sciences de Liege 43 (1974) 96-105.
[12] R.J.H. Clark, Journal of Molecular Structure 480-481 (1999) 15-20.
[13] L. Burgio, D.A. Ciomartan, R.J.H. Clark, Journal of Raman Spectroscopy 28 (1997) 79-83.
[14] M. Bouchard, D.C. Smith, Asian Chemistry Letters 5 (2001) 157-170.
[15] B. Guineau, Studies in Conservation 29 (1984) 35-41.
[16] C. Rocchiccioli, Compt. Rend. 259 (1964) 4581-4584.
[17] R.L. Frost, D.L. Wain, W.N. Martens, B.J. Reddy, Polyhedron 26 (2007) 275-283.
[18] R.L. Frost, J. Raman Spectrosc. 37 (2006) 910-921.
[19] H.H. Adler, P.F. Kerr, American Mineralogist 48 (1963) 124-137.
[20] C.K. Huang, P.F. Kerr, American Mineralogist 45 (1960) 311-324.
[21] H. Moenke, W. Zabinski, Geologie (Berlin) 12 (1963) 1221-1222.
[22] J.M. Hunt, M.P. Wisherd, L.C. Bonham, Anal. Chem. 22 (1950) 1478-1497.
[23] G.R. Hunt, J.W. Salisbury, Modern Geology 2 (1971) 23-30.
[24] W.P. Griffith, Nature (London, United Kingdom) 224 (1969) 264-266.
[25] R.G. Herman, C.E. Bogdan, A.J. Sommer, Materials Science Research 19 (1985) 113-130.
[26] W.P. Griffith, Journal of the Chemical Society [Section] A: Inorganic, Physical, Theoretical (1970) 286-291.
[27] R.S. Braithwaite, G. Ryback, Mineral. Mag. 33 (1963) 441-449.
[28] R.G. Herman, C.E. Bogdan, P.L. Kumler, D.M. Nuszkowski, Materials Chemistry and Physics 35 (1993) 233-239.
[29] J.L. Jambor, Canadian Mineralogist 8 (1964) 92-108.
[30] J.L. Jambor, I.D. MacGregor, Paper - Geological Survey of Canada 74-1, Pt. B (1974) 172-174.
[31] S. Vedanand, B.M. Sudhana, B.J. Reddy, P.S. Rao, Bulletin of Materials Science 19 (1996) 1089-1094.
[32] B.J. Reddy, F. Nieto, A.S. Navas, Neues Jahrbuch fuer Mineralogie, Monatshefte (2004) 302-316.
[33] D. Stoilova, V. Koleva, V. Vassileva, Spectrochimica Acta, Part A: Molecular and Biomolecular Spectroscopy 58A (2002) 2051-2059.
[34] R.L. Frost, S.J. Palmer, J.M. Bouzaid, B.J. Reddy, J. Raman Spectrosc. 38 (2007) 68-77.
[35] R.L. Frost, D.A. Henry, M.L. Weier, W. Martens, J. Raman Spectrosc. 37 (2006) 722-732.
[36] R.L. Frost, A.W. Musumeci, J.T. Kloprogge, M.O. Adebajo, W.N. Martens, J. Raman Spectrosc. 37 (2006) 733-741.
[37] R.L. Frost, J. Cejka, M. Weier, W.N. Martens, J. Raman Spectrosc. 37 (2006) 879-891.
[38] R.L. Frost, M.L. Weier, J. Cejka, J.T. Kloprogge, J. Raman Spectrosc. 37 (2006) 585-590.
[39] R.L. Frost, J. Cejka, M.L. Weier, W. Martens, J. Raman Spectrosc. 37 (2006) 538-551.
[40] R.L. Frost, M.L. Weier, B.J. Reddy, J. Cejka, J. Raman Spectrosc. 37 (2006) 816-821.
[41] R.L. Frost, M.L. Weier, W.N. Martens, J.T. Kloprogge, J. Kristof, J. Raman Spectrosc. 36 (2005) 797-805.
[42] R.L. Frost, R.-A. Wills, M.L. Weier, W. Martens, J. Raman Spectrosc. 36 (2005) 435-444.
[43] R.L. Frost, D.A. Henry, K. Erickson, J. Raman Spectrosc. 35 (2004) 255-260.
[44] R.L. Frost, Spectrochim. Acta, Part A 60A (2004) 1469-1480.
[45] R.L. Frost, O. Carmody, K.L. Erickson, M.L. Weier, J. Cejka, J. Mol. Struct. 703 (2004) 47-54.

[46] R.L. Frost, O. Carmody, K.L. Erickson, M.L. Weier, D.O. Henry, J. Cejka, J. Mol. Struct. 733 (2004) 203-210.
[47] A.K. Alwan, P.A. Williams, Transition Metal Chemistry (Dordrecht, Netherlands) 4 (1979) 128-132.
[48] P.A. Williams, Oxide Zone Geochemistry, Ellis Horwood Ltd, Chichester, West Sussex, England, 1990.
[49] F. Zhu, D. Persson, D. Thierry, Corrosion (Houston, TX, United States) 57 (2001) 582-590.
[50] R.L. Frost, P.A. Williams, W. Martens, Mineral. Mag. 67 (2003) 103-111.
[51] R.L. Frost, M.L. Weier, Thermochim. Acta 406 (2003) 221-232.
[52] R.L. Frost, M.L. Weier, J.T. Kloprogge, J. Raman Spectrosc. 34 (2003) 760-768.
[53] R.L. Frost, M.L. Weier, Thermochim. Acta 409 (2004) 79-85.
[54] W.N. Martens, L. Rintoul, J.T. Kloprogge, R.L. Frost, Am. Mineral. 89 (2004) 352-358.
[55] R.L. Frost, K.L. Erickson, M.L. Weier, O. Carmody, J. Cejka, J. Mol. Struct. 737 (2005) 173-181.
[56] L. Frost Ray, L. Weier Matt, J. Cejka, A. Ayoko Godwin, Spectrochimica acta. Part A, Molecular and biomolecular spectroscopy 65 (2006) 529-534.
[57] R.L. Frost, B.J. Reddy, D.L. Wain, M.C. Hales, J. Near Infrared Spectrosc. 14 (2006) 317-324.
[58] R.L. Frost, B.J. Reddy, D.L. Wain, W.N. Martens, Spectrochim. Acta, Part A 66 (2007) 1075-1081.

IR - Synthetic Smithsonite			IR - Synthetic Hydrozincite			Raman - Synthetic Smithsonite			Raman - Synthetic Hydrozincite		
Center	**FWHM**	**%**	**Center**	**FWHM**	**%**	**Center**	**FWHM**	**%**	**Center**	**FWHM**	**%**
			3478	189	6.07				3541	137	3.01
						3472	234	12.92			
									3407	142	17.06
3356	310	7.26									
			3291	282	31.44				3286	251	29.67
						3265	288	8.86			
			3063	222	4.74						
									2934	131	1.71
			2895	231	3.83						
2498	32	0.28									
									2330	3	0.10
1813	29	0.24									
						1734	10	1.71			
									1692	58	0.61
									1545	17	0.97
									1532	74	2.37
			1505	81	16.05						
1474	96	16.87									
1424	67	14.84				1408	10	6.03			
1392	43	30.44	1383	65	8.12				1380	77	1.61
									1370	15	1.91
1367	43	11.78									
1344	220	5.74	1338	59	8.12						
1330	57	6.54									
						1092	9	33.57			
									1078	15	0.47
			1060	119	3.20				1062	15	9.40
			1042	23	0.96				980	19	0.35
			949	69	2.28						
864	14	4.60	888	51	1.76						
834	34	1.87	832	20	2.64						
			799	93	2.25				801	294	7.72
743	7	1.37	737	16	0.25	730	6	1.98	733	20	2.37
715	88	2.07	707	10	0.32				707	9	0.76
			693	103	7.73						
			626	45	0.24				636	41	0.74
									417	244	10.71
									385	18	3.02
						350	453	11.90	346	43	2.18
						304	15	19.83			
									272	38	0.95
									227	33	1.49
						198	12	3.21	198	38	0.52

Table 1 Results of the Raman and infrared spectra of synthetic smithsonite and hydrozincite

List of Figures

List of Tables

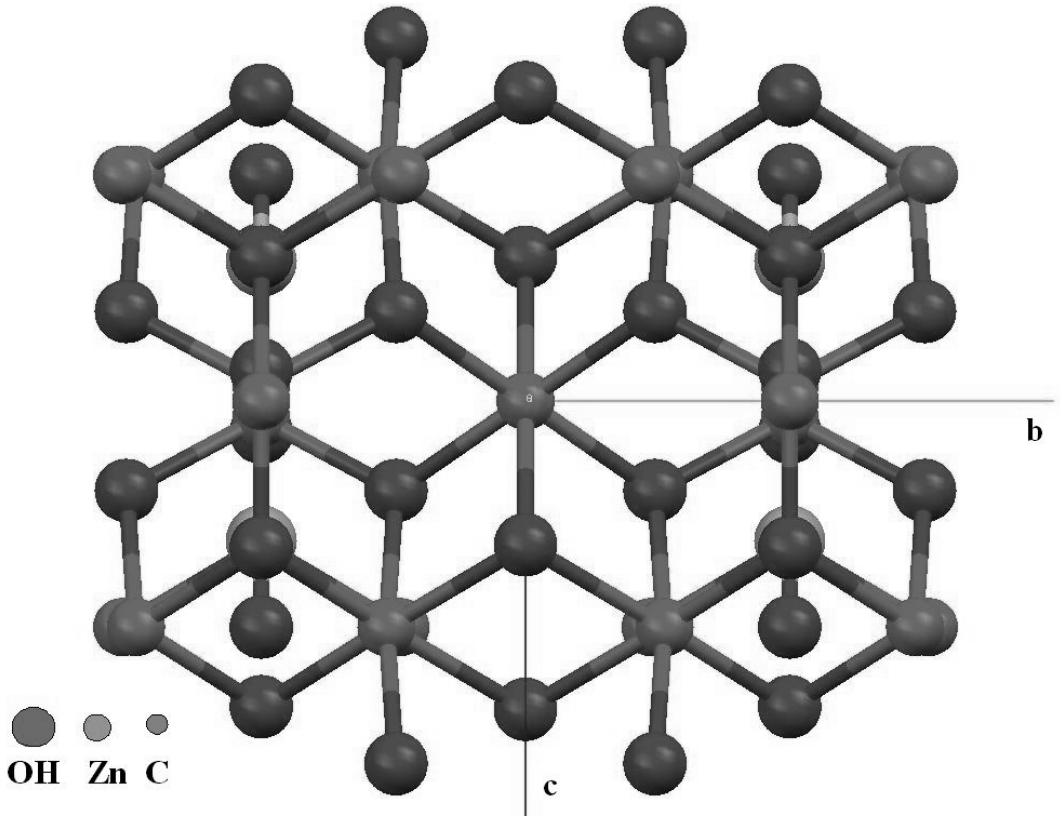

Figure 1a along a axis

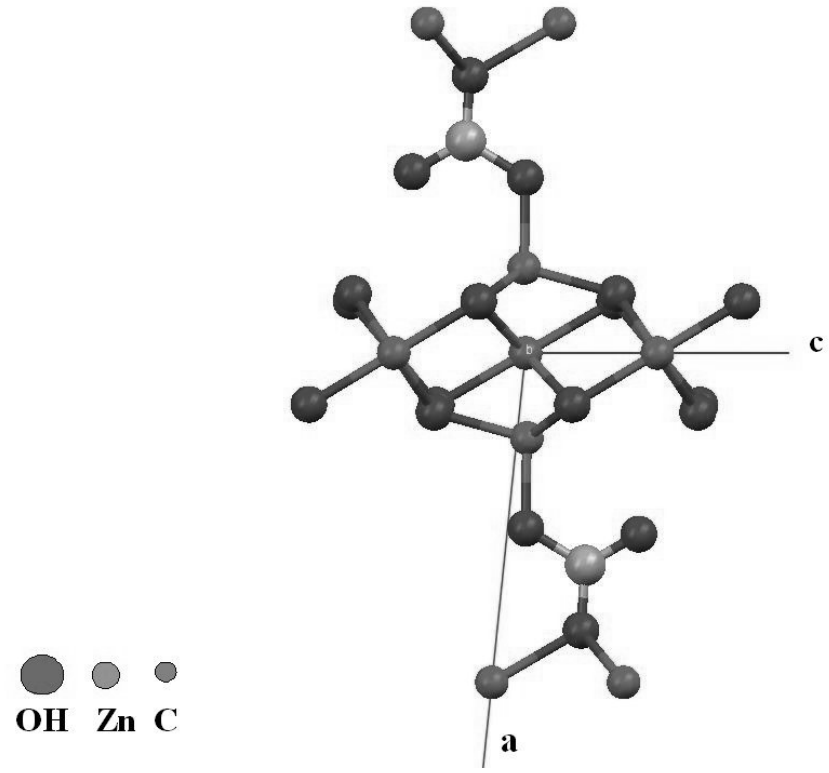

Figure 1b along b axis

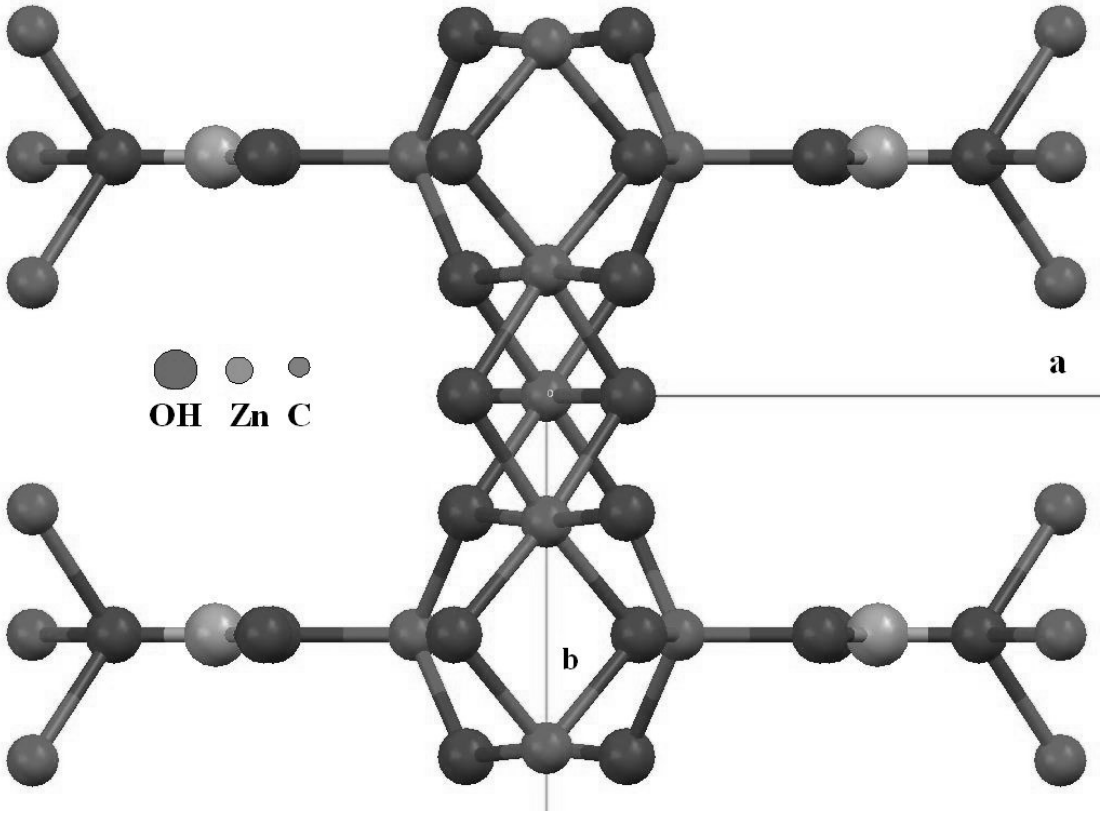

Figure 1c along c axis

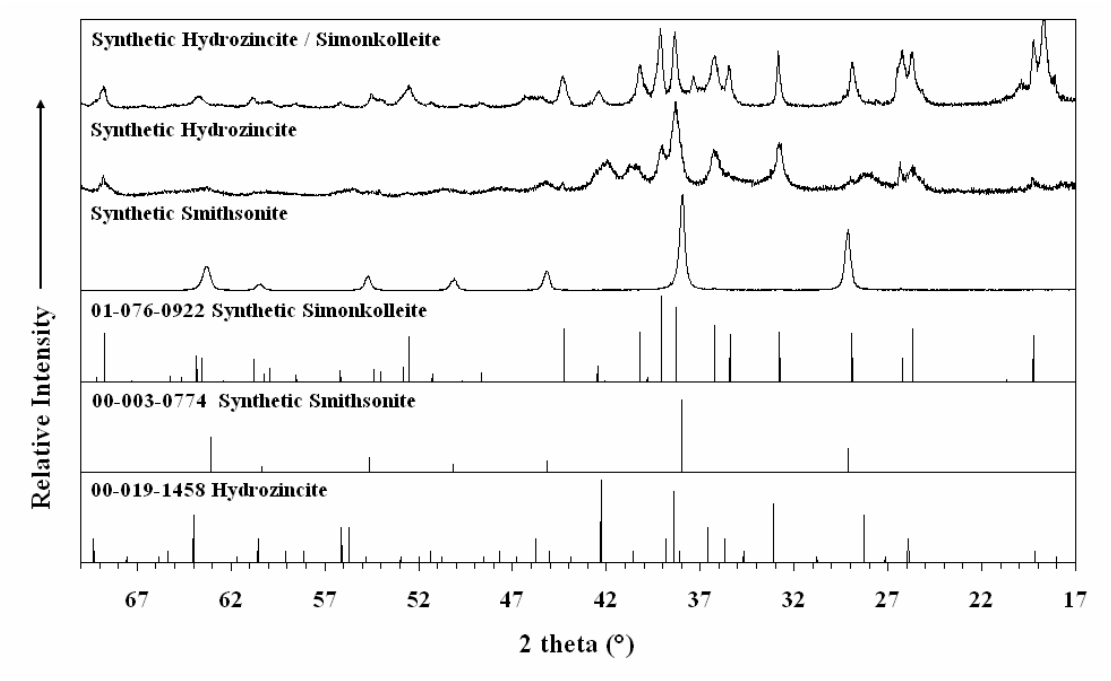
Synthetic Hydrozincite / Simonkolleite
Synthetic Hydrozincite
Synthetic Smithsonite
01-076-0922 Synthetic Simonkolleite
00-003-0774 Synthetic Smithsonite
00-019-1458 Hydrozincite
Relative Intensity
67
62
57
52
47
42
37
32
27
22
17
2 theta (°)

Figure 2

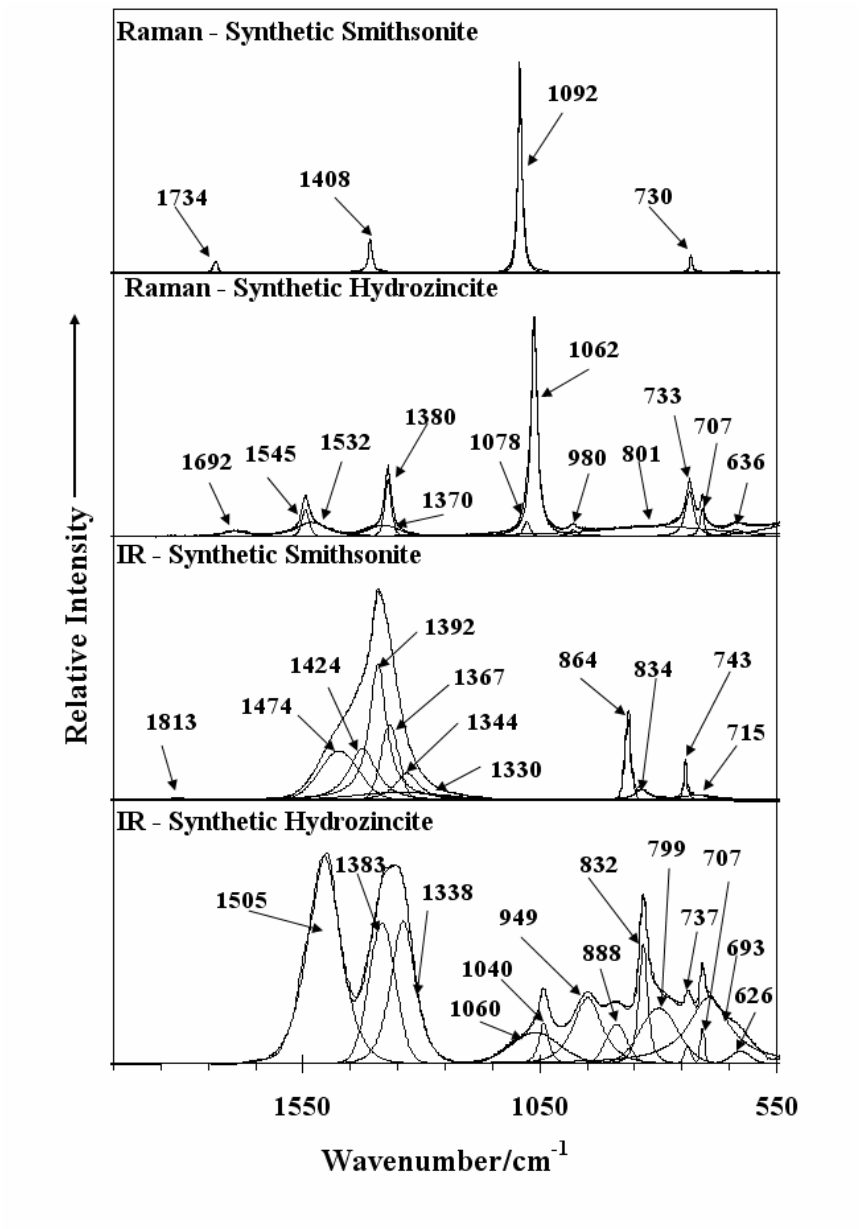
Raman - Synthetic Smithsonite
1092
1734
1408
730
Raman - Synthetic Hydrozincite
1062
733
1380
707
1692
1545
1532
1078
980
801
636
1370
IR - Synthetic Smithsonite
1392
1424
1367
864
834
743
1474
1813
1344
715
1330
IR - Synthetic Hydrozincite
1383
832
799
707
1505
1338
949
737
888
693
1040
626
1060
Relative Intensity
1550
1050
550
Wavenumber/cm-1

Figure 3

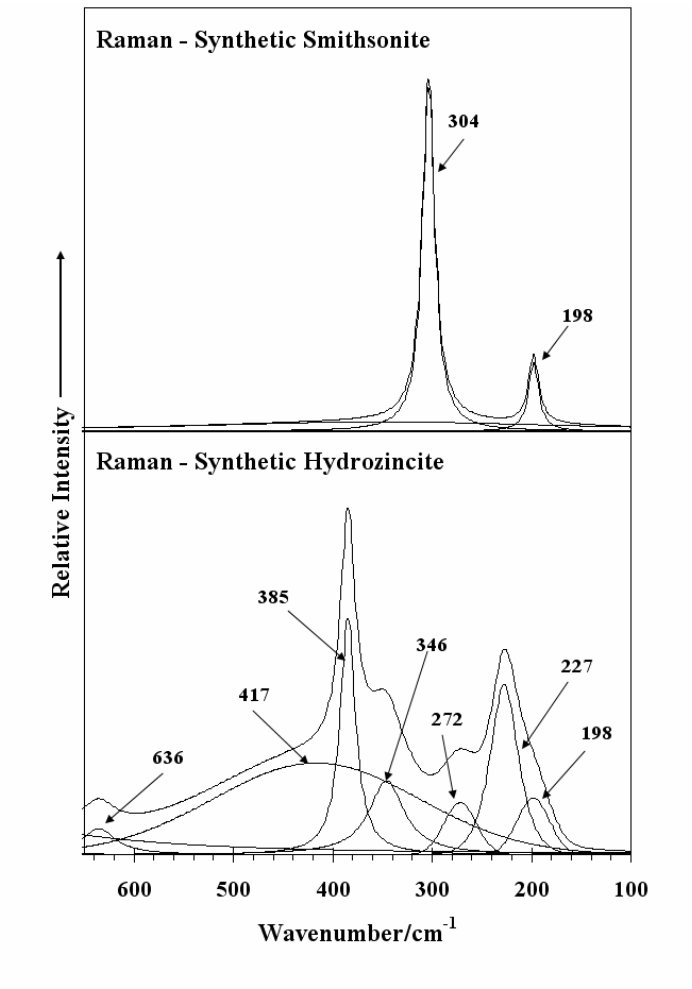
Raman - Synthetic Smithsonite
304
198
Raman - Synthetic Hydrozincite
385
346
227
417
272
198
636
Relative Intensity
600
500
400
300
200
100
Wavenumber/cm-1

Figure 4

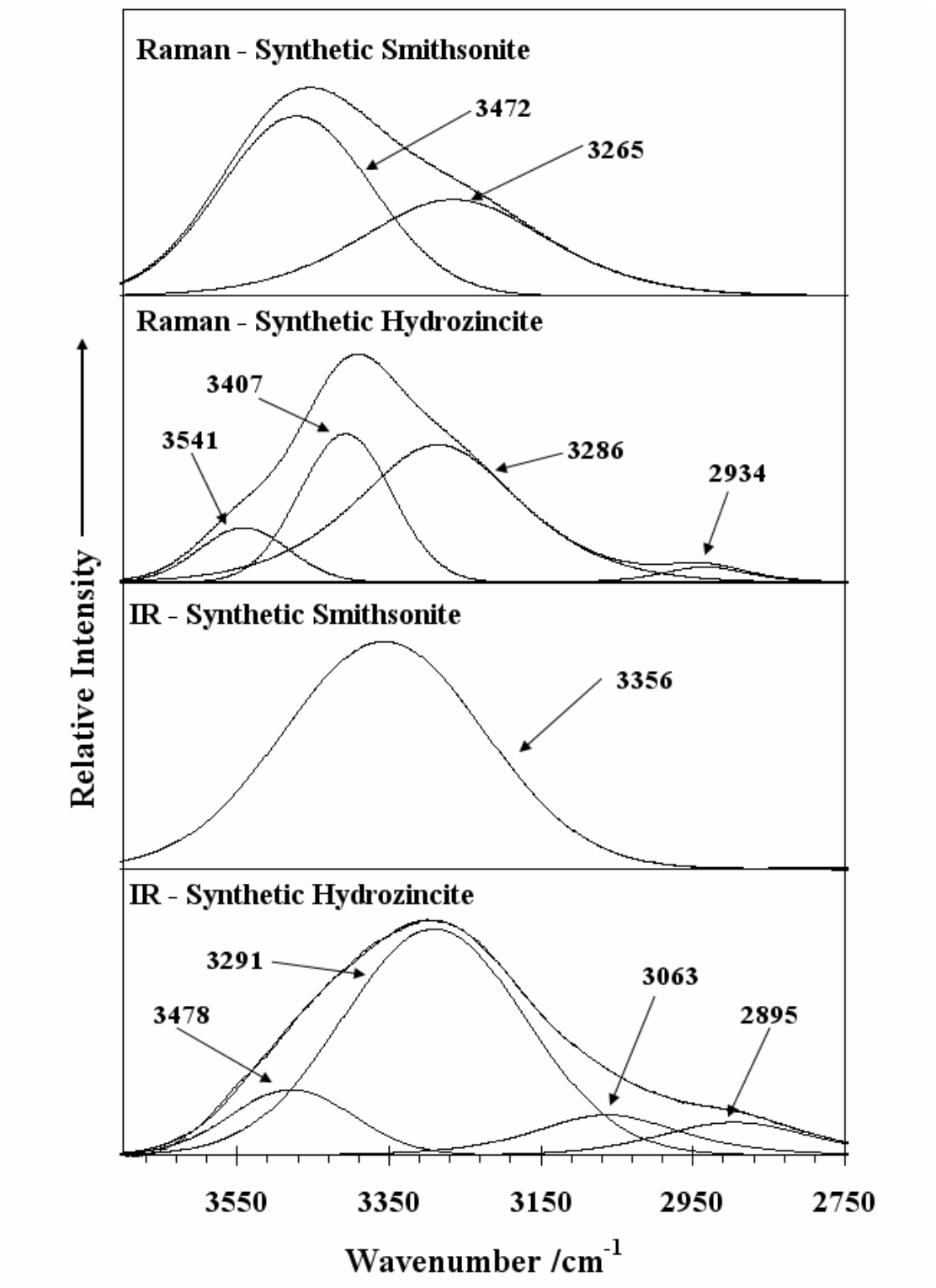
Raman - Synthetic Smithsonite
3472
3265
Raman - Synthetic Hydrozincite
3407
3541
3286
2934
IR - Synthetic Smithsonite
3356
IR - Synthetic Hydrozincite
3291
3063
3478
2895
Relative Intensity
3550
3350
3150
2950
2750
Wavenumber /cm-1

Figure 5